ISSN 1063-7710, Acoustical Physics, 2016, Vol. 62, No. 2, pp. 160–164. © Pleiades Publishing, Ltd., 2016.

NONLINEAR ACOUSTICS

Nonlinear Thickness-Stretch Vibration of Thin-Film Acoustic Wave Resonators[1]

Xiaojun Ji, Yanping Fan, Tao Han, and Ping Cai

Department of Instrument Science and Engineering Shanghai Jiao Tong University, Shanghai 200240, China

e-mail: jxj127@sjtu.edu.cn

Received August 30, 2014

Abstract—We perform a theoretical analysis on nonlinear thickness-stretch free vibration of thin-film acoustic wave resonators made from AlN and ZnO. The third-order or cubic nonlinear theory by Tiersten is employed. Using Green's identify, under the usual approximation of neglecting higher time harmonics, a perturbation analysis is performed from which the resonator frequency-amplitude relation is obtained. Numerical calculations are made. The relation can be used to determine the linear operating range of these resonators. It can also be used to compare with future experimental results to determine the relevant third- and/or fourth-order nonlinear elastic constants.

Keywords: acoustic wave resonator; nonlinear thickness-stretch free vibration; thin film

DOI: 10.1134/S1063771016020159

1. INTRODUCTION

Piezoelectric crystal resonators are now widely used as frequency generators and duplexers in telecommunication system. They are made from crystals with low damping (high Q) and operating in resonant conditions. With the increasing demand for the power durability in front ends of mobile handsets [1, 2], crystal resonators may be driven into nonlinear range in strong vibrations with relatively larger deformations. This has a series of implications in various nonlinear effects, such as frequency-amplitude dependence, anisochronism, higher harmonic generation, and intermodulation, etc., which are usually considered undesirable. To determine the linear operation range, nonlinear analyses on resonator behaviors are necessary. For older crystal resonator materials like quartz, nonlinear analyses on resonator near resonances were performed in, e.g., [3–6]. In particular, from the frequency-amplitude relation in [4], a fourth-order elastic constant of AT-cut quartz, c_{6666} in the Voigt (or compressed matrix) notation, was obtained which is the most useful one among the fourth-order elastic constants of quartz. For newer resonator materials like AlN and ZnO which are of current interest in making thin-film bulk acoustic wave resonators (FBARs) [7], while there are extensive results in the literature from linear analyses, there seems to be few reports on nonlinear analysis. In addition to the lack of basic understanding of nonlinear behaviors in FBARs, the relevant fourth-order nonlinear material constant, c_{3333}, seems to be currently unavailable for both AlN and ZnO. For ZnO, even the relevant third-order elastic constant, c_{333}, cannot be found. In this paper, based on the third-order nonlinear theory by Tiersten [8], we perform a theoretical analysis on nonlinear thickness-stretch free vibration of thin-film acoustic wave resonators to obtain their basic nonlinear vibration characteristics which have various applications.

2. GOVERNING EQUATIONS

We use the third-order theory for nonlinear motions of electroelastic solids valid for weak mechanical nonlinearities. The equations of motion and the charge (or Gauss) equation of electrostatics are [9]

$$K_{LM,L} = \rho \ddot{\tilde{u}}_M, \quad D_{L,L} = 0, \tag{1}$$

where the Cartesian tensor notion is used. $\tilde{u}_M$ is the displacement vector, K_{LM} is the first Piola-Kirchhoff stress which is asymmetric in general, and D_L is the reference or material electric displacement vector. The constitutive relations are [8]

$$\begin{aligned} K_{LM} &= c_{LMRS}\tilde{u}_{R,S} + e_{RLM}\tilde{\varphi}_{,R} + \frac{1}{2}c_{LMRS}\tilde{u}_{K,R}\tilde{u}_{K,S} \\ &+ c_{LKRS}\tilde{u}_{M,K}\tilde{u}_{R,S} + \frac{1}{2}c_{LMRSNJ}\tilde{u}_{R,S}\tilde{u}_{N,J} \\ &+ \frac{1}{2}c_{LBRS}\tilde{u}_{M,B}\tilde{u}_{K,R}\tilde{u}_{K,S} + \frac{1}{2}c_{LKRSNJ}\tilde{u}_{M,K}\tilde{u}_{R,S}\tilde{u}_{N,J} \\ &+ \frac{1}{2}c_{LMRSNJ}\tilde{u}_{R,S}\tilde{u}_{K,N}\tilde{u}_{K,J} + \frac{1}{6}c_{LMRSNJEF}\tilde{u}_{R,S}\tilde{u}_{N,J}\tilde{u}_{E,F}, \\ D_L &= e_{LNK}\tilde{u}_{N,K} - \varepsilon_{LK}\tilde{\varphi}_{,K}, \end{aligned} \tag{2}$$

[1] The article is published in the original.

where $\tilde{\varphi}$ is the electric potential; c_{LMRS}, e_{RLM} and ε_{LK} are the usual elastic, piezoelectric, and dielectric constants; c_{LMRSNJ} and $c_{LMRSNJEF}$ are the third- and the fourth-order elastic constants responsible for nonlinear material behaviors. They are in Cartesian tensor notation. Because the linear oscillatory behavior is essentially elastic, it is reasonable to assume that the nonlinear interaction is purely elastic and that the electro-elastic interaction is due to linear piezoelectricity [10]. Since the major nonlinearity in crystal resonators is from mechanical origins, the second equation in Eq. (2) is kept linear. Electrical nonlinearities are neglected as an approximation.

Consider the FBAR in Fig. 1. The six-fold axis of AlN (or ZnO) is along X_3. It is electroded at its two surfaces and can be driven into thickness-stretch vibration by a thickness electric field produced by an applied voltage across the electrodes. We are interested in free vibration frequencies for which the applied voltage will be set to zero. For thickness-stretch motions we have

$$\tilde{u}_1 = \tilde{u}_2 = 0,\ \tilde{u}_3 = \tilde{u}(x_3, t),\quad \tilde{\varphi} = \tilde{\varphi}(x_3, t). \tag{3}$$

The relevant equation of motion, charge equation, and constitutive relations take the following form:

$$K_{33,3} = \rho\ddot{\tilde{u}}_3,\quad D_{3,3} = 0, \tag{4}$$

$$K_{33} = c_{33}\tilde{u}_{3,3} + e_{33}\tilde{\varphi}_{,3} + \left(\frac{3}{2}c_{33} + \frac{1}{2}c_{333}\right)(\tilde{u}_{3,3})^2 + \left(\frac{1}{2}c_{33} + c_{333} + \frac{1}{6}c_{3333}\right)(\tilde{u}_{3,3})^3, \tag{5}$$

where the Voigt notation for the material constants is used. The boundary conditions for traction-free surfaces and shorted electrodes are

$$K_{33} = 0,\ \tilde{\varphi} = 0,\ \text{at } x_3 = \pm h. \tag{6}$$

3. LINEAR SOLUTION

Our analysis of the nonlinear thickness-stretch vibration of FBARs will be based on a perturbation analysis from the linear solution. For later use, in this section summarize the linear solution below. For the linear solution we denote the relevant displacement and potential by u_3 and φ. They are governed by (4–6) with $c_{333} = 0$ and $c_{3333} = 0$. For free vibration with shorted electrodes, the relevant displacement solution of symmetric modes can be found from [11] and [12] as

$$u_3 = A\sin\xi x_3\cos\omega_0 t, \tag{7}$$

where A is an arbitrary constant. Physically it represents the vibration amplitude or the plate surface displacement. The resonant frequency ω_0 is determined from the following frequency equation:

$$\xi h\cot\xi h = \bar{k}_{33}^2, \tag{8}$$

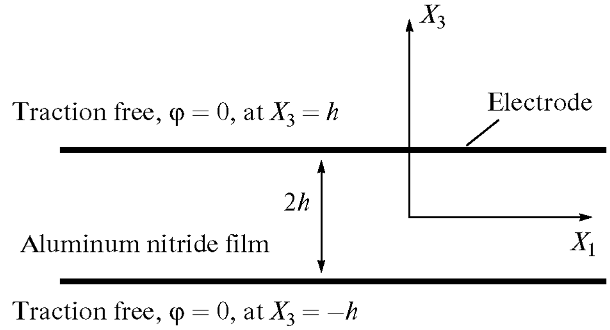

Fig. 1. Schematic diagram of an FBAR.

where

$$\xi^2 = \frac{\rho}{\bar{c}_{33}}\omega_0^2,\ \bar{c}_{33} = c_{33}(1 + k_{33}^2),\quad k_{33}^2 = \frac{e_{33}^2}{\varepsilon_{33}c_{33}},\ \bar{k}_{33}^2 = \frac{e_{33}^2}{\varepsilon_{33}\bar{c}_{33}} = \frac{k_{33}^2}{1 + k_{33}^2}. \tag{9}$$

Equation (8) in fact determines a series of resonant frequencies. For a plate with $h = 1$ μm, using the second-order material parameters for linear behaviors of AlN in [13, 14] and of ZnO in [15, 16], the fundamental thickness-stretch frequency is found to be

$$\omega_0 = \sqrt{\frac{\bar{c}_{33}}{\rho}}\xi = \begin{cases} 16.334 \times 10^9 \text{ rad/s, AlN}, \\ 9.5471 \times 10^9 \text{ rad/s, ZnO}. \end{cases} \tag{10}$$

4. NONLINEAR ANALYSIS

For nonlinear thickness-stretch vibration governed by (4)–(6), we begin with

$$\tilde{u}_1 = \tilde{u}_2 = 0,\ \tilde{u}_3 = \tilde{u}(x_3)\cos\omega t,\quad \tilde{\varphi} = \tilde{\varphi}(x_3)\cos\omega t. \tag{11}$$

Substituting (11) into (4), and then eliminating $\tilde{\varphi}$, we obtain the following equation for $\tilde{u}_3$ from the first equation in(4):

$$\bar{c}_{33}\tilde{u}_{,33}\cos\omega t + \left(\frac{3}{2}c_{33} + \frac{1}{2}c_{333}\right)\tilde{u}_{,3}\tilde{u}_{,33}(1 + \cos 2\omega t) + \frac{3}{4}\left(\frac{1}{2}c_{33} + c_{333} + \frac{1}{6}c_{3333}\right)(\tilde{u}_{,3})^2\tilde{u}_{,33}(3\cos\omega t + \cos 3\omega t) = -\rho\omega^2\tilde{u}\cos\omega t. \tag{12}$$

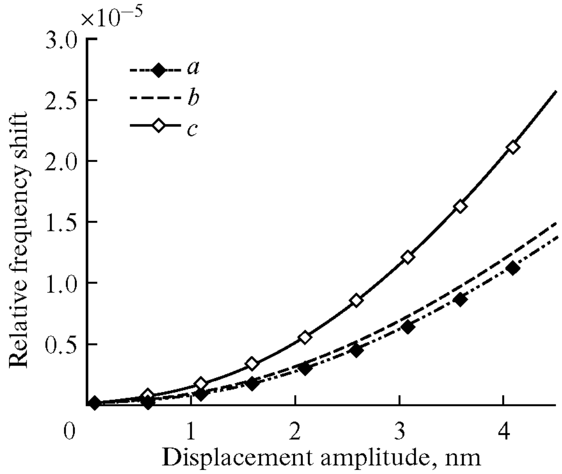

Fig. 2. Frequency-amplitude relation for AlN, symmetric mode. Line *a*: $c_{3333} = 0$; line *b*: $c_{3333} = c_{333}$; line *c*: $c_{3333} = 10\,c_{333}$.

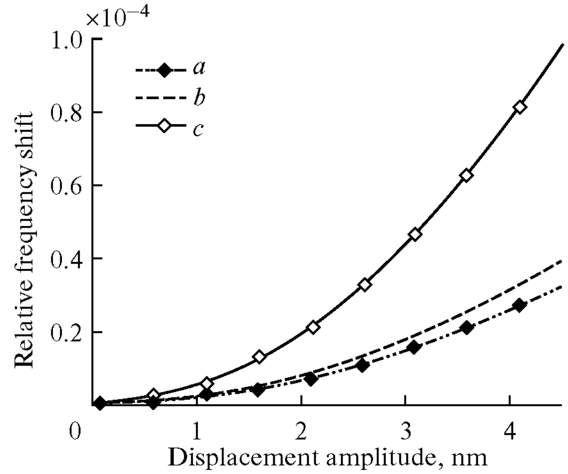

Fig. 3. Frequency-amplitude relation for ZnO, symmetric mode. Line *a*: $c_{3333} = 0$; line *b*: $c_{3333} = c_{333}$; line *c*: $c_{3333} = 10c_{333}$.

We neglect the second and the third time harmonics which is a common approximation in this type of analyses [3, 6]. Then (12) becomes

$$\bar{c}_{33}\tilde{u}_{,33}\cos\omega t + \left(\frac{3}{2}c_{33} + \frac{1}{2}c_{333}\right)\tilde{u}_{,3}\tilde{u}_{,33} + \frac{9}{4}\left(\frac{1}{2}c_{33} + c_{333} + \frac{1}{6}c_{3333}\right)(\tilde{u}_{,3})^2\tilde{u}_{,33}\cos\omega t = -\rho\omega^2\tilde{u}(x_3)\cos\omega t. \quad (13)$$

We then differentiate both sides of (13) with respect to time and eliminate the common time-dependent factor from every term. This gives

$$\bar{c}_{33}\tilde{u}_{,33} + \frac{9}{4}\left(\frac{1}{2}c_{33} + c_{333} + \frac{1}{6}c_{3333}\right)(\tilde{u}_{,3})^2\tilde{u}_{,33} = -\rho\omega^2\tilde{u}(x_3). \quad (14)$$

The linear solution satisfies a similar equation which can be obtained from (14) by dropping the nonlinear term, i.e.

$$\bar{c}_{33}u_{,33} = -\rho\omega_0^2 u. \quad (15)$$

Next we multiply (14) and (15) by u and $\tilde{u}$, respectively, and subtract the resulting equations from each other. This operation is in the same spirit as using Green's identity in the perturbation analysis for frequency shifts in resonators in [17] and it results in

$$\bar{c}_{33}(\tilde{u}_{,33}u - u_{,33}\tilde{u}) + \frac{9}{4}\left(\frac{1}{2}c_{33} + c_{333} + \frac{1}{6}c_{333}\right)(\tilde{u}_{,3})^2\tilde{u}_{,33}u + \rho(\omega^2 - \omega_0^2)\tilde{u}u = 0. \quad (16)$$

Finally, we approximate $\tilde{u}$ by u in (16) and integrate the equation through the plate thickness. This leads to

$$\omega^2 - \omega_0^2 = \frac{\frac{9}{16}\left(\frac{1}{2}c_{33} + c_{333} + \frac{1}{6}c_{3333}\right)A^2\xi^4\left(h - \frac{\sin 4\xi h}{4\xi}\right)}{\rho\left(h - \frac{\sin 2\xi h}{2\xi}\right)} \quad (17)$$

Eq. (17) shows the frequency-amplitude relation between ω and A which is characteristic in nonlinear vibrations. From (17) we obtain the following expression for the frequency shift $\Delta\omega = \omega - \omega_0$ arising from small mechanical nonlinearities as

$$\frac{\Delta\omega}{\omega_0} = \frac{\frac{9}{32}A^2\xi^4\left(\frac{1}{2}c_{33} + c_{333} + \frac{1}{6}c_{3333}\right)\left(h - \frac{\sin 4\xi h}{4\xi}\right)}{\omega_0^2\rho\left(h - \frac{\sin 2\xi h}{2\xi}\right)}. \quad (18)$$

We plot (18) for AlN in Fig. 2 using its ω_0 in (10). Its third-order elastic constant c_{333} can be found [18] with the value 187 GPa. Its fourth-order elastic constant c_{3333} seems to be unavailable. Different values of c_{3333} are used in the figure. Clearly, the effect of c_{3333} is significant. Figure 2 can be used to compare with experimental results in the future when available to determine c_{3333} in the manner of [4]. When the amplitude $A = 2$ nm, the relative frequency shift is of the order of 10^{-5}.

For ZnO, its third-order elastic constant c_{333} can be found [19] with the value –622.4 GPa. We are not able to find its relevant fourth-order elastic constant c_{3333}. We plot Fig. 3 using different values of c_{3333}. The behavior is similar to that in Fig. 2. Figure 3 can be

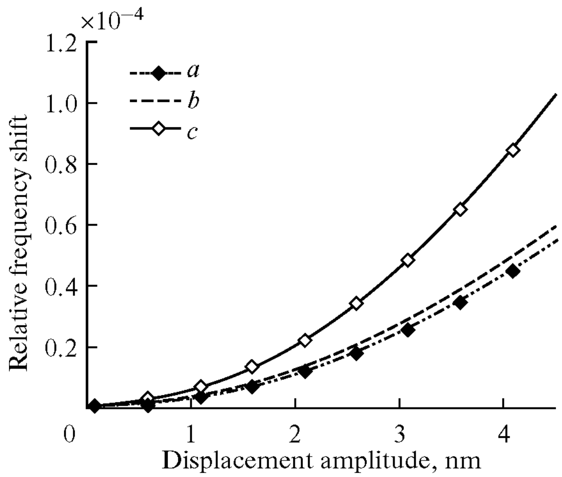

Fig. 4. Frequency-amplitude relation for AlN, anti-symmetric mode. Line *a*: $c_{3333} = 0$; line *b*: $c_{3333} = c_{333}$; line *c*: $c_{3333} = 10\, c_{333}$.

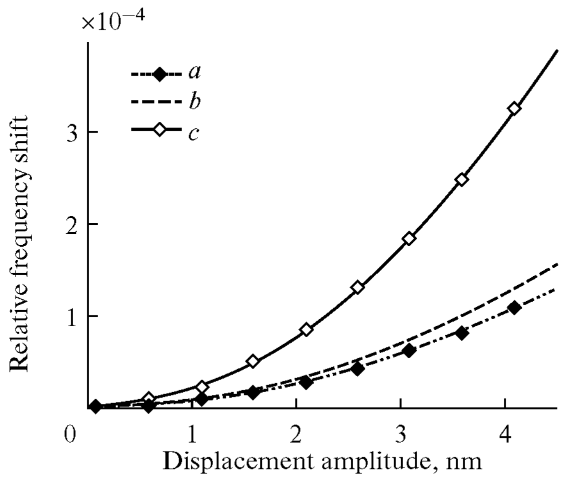

Fig. 5. Frequency-amplitude relation for ZnO, anti-symmetric mode. Line *a*: $c_{3333} = 0$; line *b*: $c_{3333} = c_{333}$; line *c*: $c_{3333} = 10\, c_{333}$.

used to compare with experimental results to determine the fourth-order elastic constant.

If we take the anti-symmetric modes of vibration for which

$$u_3 = A_2 \sin\xi x_3 \cos\omega_0 t \tag{19}$$

and

$$\xi h = n\pi,\ n = 0, 1, 2, 3, \ldots, \tag{20}$$

the fundamental frequency can be obtained as

$$\omega_0 = \sqrt{\frac{\bar{c}_{33}}{\rho}}\xi = \begin{cases} 33.617 \times 10^9 \text{ rad/s, AlN}, \\ 19.782 \times 10^9 \text{ rad/s, ZnO}. \end{cases} \tag{21}$$

Then the frequency shift $\Delta\omega = \omega - \omega_0$ arising from small mechanical nonlinearities as

$$\frac{\Delta\omega}{\omega_0} = \frac{\frac{9}{32}A^2\xi^4\left(\frac{1}{2}c_{33} + c_{333} + \frac{1}{6}c_{3333}\right)\left(h - \frac{\sin 4\xi h}{4\xi}\right)}{2\omega_0^2\rho\left(h + \frac{\sin 2\xi h}{2\xi}\right)}. \tag{22}$$

We plot (22) for AlN and ZnO in Fig. 4 and Fig. 5, respectively.

By comparing Fig. 2 and Fig. 4, we can find that the fundamental anti-symmetric mode has a greater nonlinearity than the fundamental symmetric mode.

5. CONCLUSIONS

The frequency-amplitude relation for nonlinear thickness-stretch vibration of thin-film acoustic wave resonators is obtained through a perturbation analysis. For an AlN or ZnO resonator with a thickness of 2 μm, numerical results show that when the vibration amplitude is 2 nm the relative frequency shift is of the order of 10^{-5}. The fundamental anti-symmetric mode has a greater nonlinearity than the fundamental symmetric mode. The frequency-amplitude relation can be used to compare with experimental results for the determination of the relevant third- and/or fourth-order elastic constants.

This work was supported by the Natural Science Foundation of China under Grant Nos. 51475306 and 11474203.

REFERENCES

1. R. C. Larson, P. D. Ruby, P. D. Bradley, J. Wen, S. L. Kok, and A. Chien, in *Proc. IEEE Ultrasonics Symp., 2000*, pp. 869—874.
2. C. Collado, E. Rocas, J. Mateu, A. Padilla, and J. M. O'Callaghan, IEEE Trans. Microw. Theory Techn. **57**, 3019 (2009).
3. J. J. Gagnepain and R. Besson, in *Physical Acoustics,* Ed. by W. P. Mason and R. N. Thurston, (Academic, New York, 1975), Vol. XI.
4. H. F. Tiersten, J. Acoust. Soc. Am. **57**, 667 (1975).
5. H. F. Tiersten, J. Acoust. Soc. Am. **59**, 866 (1976).
6. J. S. Yang, X. M. Yang, J. A. Turner, J. A. Kosinski, and R. A. Pastore, Jr., IEEE Trans. Ultrason., Ferroelect., Freq. Contr., **50**, 765 (2003).
7. M. Yu. Dvoesherstov, V. I. Cherednik, S. I. Bosov, I. Ya. Orlov, and O. V. Rudenko, Acoust. Phys. **59**, 569 (2013).
8. H. F. Tiersten, J. Acoust. Soc. Am. **57**, 660 (1975).
9. V. I. Cherednik and M. Yu. Dvoesherstov, Acoust. Phys. **56**, 41 (2010).
10. J. Nosek, IEEE Trans. Ultrason., Ferroelect., Freq. Contr. **50**, 386 (2003).
11. H. F. Tiersten, J. Acoust. Soc. Am. **35** 53 (1963).

12. J. S. Yang, H. G. Zhou, Y. T. Hu, and Q. Jiang, IEEE Trans. Ultrason., Ferroelect., Freq. Contr. **52**, 1872 (2005).
13. Q. Chen, F. Li, H. Cheng, and Q. Wang, in *Proc. IEEE Int. Frequency Control Symp., 2008* pp. 609–614.
14. K. Tsubouchi, K. Sugai, and N. Mikoshiba, in *Proc. IEEE Ultrasonics Symp., 1981*, pp. 375–380.
15. G. Carlotti, G. Socino, A. Petri, and E. Verona, Appl. Phys. Lett. **51**, 1889 (1987).
16. D. F. Crisler, J. J. Cupal, and A. R. Moore, Proc. IEEE **56** 225 (1968).
17. H. F. Tiersten, J. Acoust. Soc. Am. **64**, 832 (1978).
18. M. Petrov, L. Lymperakis, J. Neugebauer, R. Stefaniuk, and P. Dluzewski, in *Proc. 17th Int. Conf. Compt. Methods Mechan., CMM, 2007.*
19. X. Wang, Y. Gu, X. Sun, H. Wang, and Y. Zhang, J. Appl. Phys. **115**, 213516 (2014).